Natural Convection Heat Transfer of the Oxide Layer in the two-layer configuration and three-layer configuration

Su-Hyeon Kim[1*] and Bum-Jin Chung[2]
[1]*SMART Reactor Design Division, Korea Atomic Energy Research Institute*
111, Daedeok-daero 989 Beon-gil, Yuseong-Gu, Daejeon, 34057, Korea
[2]*Department of Nuclear Engineering, Kyung Hee University*
#1732 Deogyeong-daero, Giheung-gu, Yongin-si, Gyeonggi-do, 17104, Korea
[*]*Corresponding author*: *sukim@kaeri.re.kr*

1. Introduction

SMART (System-integrated Modular Advanced ReacTor) is an integral type reactor developed by Korea aiming the enhanced safety and improved economics. SMART has adopted the IVR-ERVC (In-Vessel Retention-External Reactor Vessel Cooling) as a severe accident management strategy. The IVR-ERVC retains the molten corium inside the reactor vessel by cooling the external vessel wall. It is effective to maintain the vessel integrity and prevent the radioactive material release into an environment. [1] The corium is stratified into two-layer or three-layer at the lower vessel as shown in Figure 1. The heat load is focused on the vessel wall especially from the upper metal layer which is called focusing effect. Focusing effect is one of the dangerous phenomena to threaten the integrity of reactor vessel. It can be intensified in a three-layer configuration as the upper metal layer thickness is reduced due to the formation of additional heavy metal layer. However, very few studies were performed for a three-layer configuration. [2]

This study conducted the natural convection heat transfer experiments of oxide layer for a two-layer configuration and three-layer configuration in SAMRT. Mass transfer experiments were performed employing the copper sulfate–sulfuric acid ($CuSO_4$–H_2SO_4) electroplating system based on the analogy concept between heat and mass transfer. The high buoyancy with the Ra'_H ranged from 10^{11} to 10^{13} was achieved in small facilities named MassTER-OP2(HML): Mass Transfer Experimental Rig for a 2D Oxide Pool above Heavy Metal layer. Upward heat ratios measured and compared for each case. Also, local heat transfers were measured to analyze the natural convective flow patterns of oxide layer.

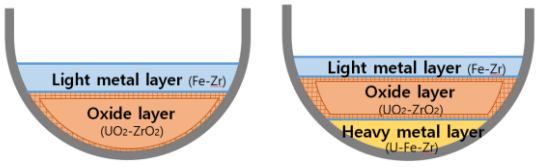

(a) two-layer (b) three-layer
Figure 1. Stratified molten pool configuration.

2. Theoretical Background

2.1 Phenomena

Molten corium is generally assumed to be stratified into two-layer as shown in Fig. 1(a). Upper layer consists of metallic materials such as Zr and Fe, and the lower layer consists of oxidized materials such as UO_2 and ZrO_2. MASCA research [3] discovered that U migrated the upper metal layer increasing the metal layer density. Then, some of metal layer containting U moved into the bottom forming the heavy metal layer as shown in Fig. 1(b). The bottom heavy metal layer cotnains U, Fe, Zr and some metallic fission products.

Figure 2 indicates flow patterns of oxide layer in the two-layer and three-layer configuration. Natural convective flows move down along the curvature and merge at the bottom. Merged flows rise to the top and then dispherse towards the edge. There are also second natural convective flows underneath the top plate. [4]

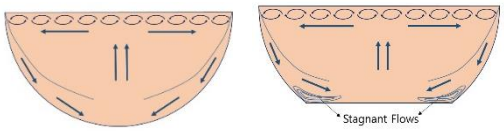

(a) two-layer (b) three-layer
Figure 2. Flow patterns.

2.2 Previous studies

2.2.1 Two-layer experiments

Previous heat transfer experiments of oxide layer for two-layer configuration were summarized in the Table 1.

Table 1. Summary of previous two-layer studies

Facility	Pool	Working fluid	Ra'_H	Correlations
BALI [4] (2D)	Semicircle	Cellulose added water	10^{13}–10^{17}	$Nu_{up}=0.383Ra'^{0.233}_H$ $Nu_{dn}=0.116Ra'^{0.25}_H$
SIGMA CP [5] (2D)	Semicircle	Water and Air	5×10^{6}–7×10^{11}	$Nu_{up}=0.31(Ra'_H Pr^{0.36})^{0.245}$ $Nu_{dn}=0.31(Ra'_H Pr^{0.215})^{0.235}$
CORPRA [6,7] (2D)	1/4 circle	Water and $NaNO_3$–KNO_3	1.2×10^{15}–4.0×10^{16}	-
ACOPO [8] (3D)	Hemisphere	Water	8×10^{13}–2×10^{16}	$Nu_{up}=1.95Ra'^{0.18}_H$ $Nu_{dn}=0.3Ra'^{0.22}_H$
UCLA [9] (3D)	Hemisphere	Water	5×10^{11}–8×10^{13}	$Nu_{up}=0.403Ra'^{0.226}_H$ $Nu_{dn}=0.54(Ra'_H)^{0.2}(H/R_e)^{0.25}$

2.2.2 Three-layer experiments

SIMECO tests [10] simulated three-layer stratification using paraffin oil (top), water (middle) and chlorobenzene (bottom) using a 2-D facility. The heights of top, middle and bottom layer were 5 cm, 18 cm and 4 cm. A 20 cm long heater was installed at the elevation of 4 cm, maintaining the bottom layer unheated. The range of Ra'_H was achieved from 6.01×10^{12} to 7.82×10^{12}. The test for a two-layer configuration was also carried out in the identical condition with the three-layer configuration except for the bottom layer. The ratio of upward heat flux to downward heat flus was higher for three-layer configuration than two-layer configuration. The angular heat fluxes increased with the angle, peaking at the middle of the oxide layer: 64 degree in the three-layer test and 57 degrees in the two-layer test. The two-layer result from this study is different with those from other two-layer studies indicating the heat flux peak at the uppermost angle of oxide layer.

Several limitations of SIMECO study are as following. (1) The tests did not focus on the oxide layer. (2) The measurements were obtained for certain section. (3) The heights of three layers were determined arbitrarily. (4) The local results in two-layer configuration were inconsistent with other existing results.

2.3 Definition of Ra'_H

The modified Rayleigh number (Ra'_H) is used intead of conventional Rayleigh number (Ra_H) to consider the internal heat generation of the oxide layer. The Ra'_H is expressed by

$$Ra'_H = Ra_H \times Da \,, \tag{1}$$

$$\text{Damköhler number } (Da) = \frac{q'''H^2}{k\Delta T} \text{ and} \tag{2}$$

$$Ra'_H = \frac{g\beta\Delta T H^3}{\alpha\nu} \times \frac{q'''H^2}{k\Delta T} = \frac{g\beta q'''H^5}{\alpha\nu k} \tag{3}$$

3. Experiments

3.1 Methodology

Mass transfer tests were conducted using the electroplating system based upon analogy concept between heat and mass transfer. *Sh* and *Sc* of mass transfer system analogy with *Nu* and *Pr* of heat transfer system.

Levich [11] has performed mass transfer experiments using the electroplating system. Mass transfer correlations in different conditions were organized by Selman. [12] Chung et al [13] carried out a lot of mass transfer experiments to establish the methodology in detail. A limiting current technique was employed to obtain the mass transfer coefficient as the concentration of copper ion is difficult to know near the cathode surface. When the potential between electrodes increases continuously, the current increases consistently. Then, it maintains constant despite the potential increase when the copper ion concentration on the cathode surface becomes zero. The current in this plateau section is the limiting current. Therefore, mass transfer coefficient (h_m) is defined as below.

$$h_m = \frac{(1-t_{Cu^{2+}})I_{\lim}}{nFC_b} \tag{4}$$

Upward buoyancy at a hot wall can be simulated as a cathode in the mass transfer system but the cold wall cannot be simulated as an anode. It is because the limiting current is not measured in the anode due to the crystallization of cupper ions. [14] Therefore we performed the tests using the facility inverted against the gravity direction so as to develop the buoyancy towards bottom of the facility and simulated the cathode as cold wall.

3.2 Experimental facility

Figure 3 shows the experimental facilities of this study, MassTER-OP2 and OP3 and MassTER-OP2(HML). We used 2-D semicircle and 3-D hemisphere facilities with three different height of 0.042 m, 0.1 m and 0.167 m for two-layer tests. The radius is same with height for all two-layer facilities. We also performed three-layer tests using 2-D semicircle facilities with chopped bottom with three different aspect ratios. Their radii are fixed 10 cm but heights are varied to 0.028 m, 0.056 m and 0.78 m which correspond to aspect ratio of 0.28, 0.56 and 0.78. The widths of all 2-D facilities are identically 4 cm. The cathode copper plates were attached on the inner wall of the top, curved side and bottom. The halves of copper electrodes are single electrodes and the other halves are piecewise electrode to measure the local current. The anode copper simulating the internal heat source is attached on the both flat side wall for 2-D facilities and located at the center of the hemisphere atmosphere. The facilities are filled with copper sulfate–sulfuric acid ($CuSO_4$–H_2SO_4) fluids. Figure 4 shows the test system circuit. The multi-meters are connected with cathode coppers in parallel to measure the limiting current of the cathode. The Ra'_H was ranged from 10^{12} to 10^{15} for the two-layer tests and from 10^{11} to 10^{12} for three-layer tests. The *Pr* is 2,014 for all tests.

Table 2 and Table 3 presents the test matrix.

(a) H=0.042 m (b) H=0.1 m (c) H=0.167 m

(d) H=0.042 m (e) H=0.1 m (f) H=0.167 m

(g) *H/R*=0.28 (h) *H/R*=0.56 (i) *H/R*=0.78

Figure 3. Experimental facility for two-layer configuration (2D and 3D) and three-layer configuration.

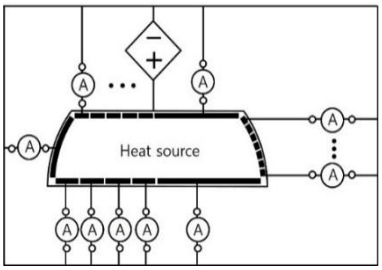

Figure 4. Experimental circuit.

Table 2. Test matrix for two-layer experiments.

	H	*Ra'$_H$*	*Top and curvature condition*	*Pr (Sc)*
MassTER-OP2	0.042 m	4.55×10^{12}	Isothermal cooling	2,014
	0.1 m	1.11×10^{14}		
	0.167 m	8.99×10^{14}		
MassTER-OP3	0.042 m	8.63×10^{12}		
	0.1 m	2.02×10^{14}		
	0.167 m	1.45×10^{15}		

Table 3. Test matrix for three-layer experiments.

	H/R	*Ra'$_H$*	*Bottom condition*	*Top and curvature condition*	*Pr (Sc)*
MassTER-OP2(HML)	0.28	7.51×10^{11}	Isothermal	Isothermal cooling	2,014
		5.76×10^{11}	Insulated		
	0.56	1.35×10^{13}	Isothermal		
		1.36×10^{13}	Insulated		
	0.78	4.30×10^{13}	Isothermal		
		3.72×10^{13}	Insulated		

4. Results and discussion

Figure 5 compares the ratios of upward heat to total heat (Q_{up}/Q_{tot}). Circles are the three-layer test results with different aspect ratios. Black closed square, star, triangle are two-layer test results in 2-D geometry with the height of 0.042 m, 0.1 m and 0.167 m. Black half closed square, star, triangle are three-layer test results in 3-D geometry with the height of 0.042 m, 0.1 m and 0.167 m. The upward heat ratios increased as the aspect ratios decreased. It is because cooling side wall is short for small aspect ratio causing a hotter rising plume towards the top plate. The two-layer results for 2-D geometry increased as the *Ra'$_H$* increase while those for 3-D geometry decreased.

All three-layer results were higher than all two-layer result. It means the three-layer configuration is more dangerous than the two-layer configuration due to intensification of focusing effect.

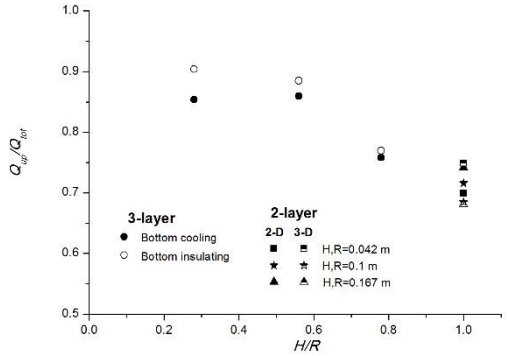

Figure 5. Upward heat ratio.

5. Conclusions

In this study, the natural convection heat transfer of oxide layer in SMART were investigated for the two-layer configuration and three-layer configuration and upward heat ratios were compared. 2-D and 3-D facilities with three different heights were employed for two-layer tests and 2-D facilities with three different aspect ratios were employed for three-layer tests. The mass transfer experiments were conducted based on the analogy concept. The upward heat ratios increased for small aspect ratio resulting the higher focusing effect of upper metal layer to the vessel. The trend of two-layer results according to Ra was different between the 2-D geometry and the 3-D geometry. Upward heat ratios for three-layer configuration are higher than those for two-layer configuration. It means the three-layer configuration are severer than two-layer configuration in terms of focusing effect.

ACKNOWLEDGMENT

This work was supported by a grant from the National Research Foundation of Korea (NRF No. 2016M2C6A 1004894) funded by the Korea government (MSIT).

REFERENCES

[1] J. L. Rempe, K. Y. Shu, F. B. Cheung, S. B. Kim, In-vessel retention of molten corium: lessons learned and outstanding issues, Nuclear technology Vol. 161, pp. 210-267, 2008.
[2] R. J. Park et al., Corium behavior in the lower plenum of the reactor vessel under IVR-ERVC condition: technical issues, Nuclear Engineering and Technology, Vol. 44, pp.237-248, 2012.

[3] M. Barrachin and F. Defoort, Thermophysical properties of In-Vessel Corium: MASCA Programme Related Results, Proceedings of MASCA Seminar 2004, Aix-en-Provence, France, 2004.
[4] J. M. Bonnet and J.M. Seiler, Thermal hydraulic phenomena in corium pools: The BALI experiment, 7th International Conference on Nuclear Engineering, Tokyo, Japan, 1999.
[5] J. K. Lee et al., Experimental study of natural convection heat transfer in a volumetrically heated semicircular pool, Annals of Nuclear Energy, Vol.73, pp. 432-440, 2014.
[6] Zhang et al., Natural convection heat transfer test for in-vessel retention at prototypic Rayleigh numbers–Results of COPRA experiments, Progress in Nuclear Energy, Vol. 86, pp. 80–86, 2016.
[7] Zhang et al., The COPRA experiments on the in-vessel melt pool behavior in the RPV lower head, Annals of Nuclear Energy, Vol. 89, pp. 19–27, 2016.
[8] Theofanous T.G., et al., The first results from the ACOPO experiment, Nuclear Engineering and Design, Vol. 169, pp. 49-57, 1997.
[9] Asfia, F.J. and Dhir, V.K., An experimental study of natural convection in a volumetrically heated spherical pool bounded on top with a rigid wall, Nuclear Engineering and Design, Vol. 163, pp. 333–348, 1996.
[10] B. R. Sehgal et al., Natural convection heat transfer in a stratified melt pool with volumetric heat generation, 6th International topical meeting on nuclear reactor thermal hydraulics, operations and safety (NUTHOS-6), Nara, Japan, 2004.
[11] V. G. Levich, Physicochemical Hydrodynamics, Prentice Hall, Englewood Cliffs & NJ, 1962.
[12] J. R. Selman, et al., Advances in Chemical Engineering, 10th, Academic Press, New York and London, 1978.
[13] B. J. Ko, W.J. Lee, B.J. Chung, Turbulent mixed convection heat transfer experiments in a vertical cylinder using analogy concept, Nuclear Engineering Design, Vol. 240, pp. 3967-3973, 2010.
[14] Y. Konishi et al., Anodic dissolusion phenomena accompanying supersaturation of copper sulfate along a vertical plane copper anode, Electrochimica Acta, 48, 2615-2624, 2003.